1993-02-01

The integral membrane protein, ponticulin, acts as a monomer in nucleating actin assembly

C. P. Chia

Et al.

The Integral Membrane Protein, Ponticulin, Acts as a Monomer in Nucleating Actin Assembly

Catherine P. Chia, Aneesa Shariff, Sharon A. Savage, and Elizabeth J. Luna

Worcester Foundation for Experimental Biology, Shrewsbury, Massachusetts 01545

Abstract. Ponticulin, an F-actin binding transmembrane glycoprotein in *Dictyostelium* plasma membranes, was isolated by detergent extraction from cytoskeletons and purified to homogeneity. Ponticulin is an abundant membrane protein, averaging $\sim 10^6$ copies/cell, with an estimated surface density of ~ 300 per μm^2. Ponticulin solubilized in octylglucoside exhibited hydrodynamic properties consistent with a ponticulin monomer in a spherical or slightly ellipsoidal detergent micelle with a total molecular mass of 56 ± 6 kD.

Purified ponticulin nucleated actin polymerization when reconstituted into *Dictyostelium* lipid vesicles, but not when a number of commercially available lipids and lipid mixtures were substituted for the endogenous lipid. The specific activity was consistent with that expected for a protein comprising 0.7 ± 0.4%, by mass, of the plasma membrane protein. Ponticulin in octylglucoside micelles bound F-actin but did not nucleate actin assembly. Thus, ponticulin-mediated nucleation activity was sensitive to the lipid environment, a result frequently observed with transmembrane proteins. At most concentrations of *Dictyostelium* lipid, nucleation activity increased linearly with increasing amounts of ponticulin, suggesting that the nucleating species is a ponticulin monomer. Consistent with previous observations of lateral interactions between actin filaments and *Dictyostelium* plasma membranes, both ends of ponticulin-nucleated actin filaments appeared to be free for monomer assembly and disassembly. Our results indicate that ponticulin is a major membrane protein in *Dictyostelium* and that, in the proper lipid matrix, it is sufficient for lateral nucleation of actin assembly. To date, ponticulin is the only integral membrane protein known to directly nucleate actin polymerization.

MEMBRANE-associated actin assembly has been proposed as the driving force behind many motile processes, including pseudopod extension (1, 22, 94, 96), microvillar elongation (64), translocation of cell surface components (35, 43), and the intracellular spread of invasive bacteria (26, 95). Newly assembled actin filaments become associated with the cell periphery within 2 to 6 s after chemotactic stimulation of neutrophils and *Dictyostelium* amebas (22, 29, 68), and actin assembly at the cytoplasmic membrane surface has been observed in living cells (34, 67, 89, 90, 94, 99).

Membrane-mediated actin assembly has been characterized in vitro using purified plasma membranes from the cellular slime mold, *Dictyostelium discoideum* (39, 59). These membranes both bind F-actin and nucleate actin polymerization at the membrane surface (57, 77, 78, 80). Binding is specific, saturable, rapid, and of high avidity, with estimated K_d's in the submicromolar range (47, 77, 88). Actin assembly appears to involve the generation of membrane-associated actin trimers (78) with both the barbed and pointed ends free to elongate (80). A 17-kD glycoprotein called ponticulin has been implicated in both actin binding and nucleation although the nature of the nucleating species is unknown (58, 80, 103).

Ponticulin apparently serves as a transmembrane link between the cell surface and the cytoskeleton. Extracellular sites have been identified by surface labeling of intact cells and Con A binding (103). A cytoplasmic domain is indicated by the continued recognition of ponticulin by antibody that has been exhaustively adsorbed against intact cells (103). Ponticulin appears to be responsible for most of the basal actin-binding activity of *Dictyostelium* plasma membranes because 96% of the actin-membrane binding in sedimentation assays is inhibited by univalent antibody fragments against the cytoplasmic domain (103). The plasma membrane localization and cytoskeletal association of ponticulin in *Dictyostelium* amebas and human neutrophils also have been demonstrated using immunofluorescence microscopy (104).

Direct binding between ponticulin and F-actin has been shown by F-actin affinity chromatography (103) and on ^{125}I-

Portions of this work were presented at the 29th and 30th Annual Meetings of the American Society for Cell Biology; Houston, TX, November 5-9, 1989 and San Diego, CA, December 9-13, 1990.

Dr. Chia's present address is the School of Biological Sciences, University of Nebraska at Lincoln, 348 Manter Hall, Lincoln, NE 68588-0118. Ms. Savage's present address is Given, Box 259, College of Medicine, University of Vermont, Burlington, VT 05405. Drs. Chia and Shariff contributed equally to the work presented in this article.

labeled F-actin blot overlays with SDS gel-purified ponticulin (16). Ponticulin–actin binding in both assays resembles actin binding to purified plasma membranes in that all these interactions are sensitive to high salt, heat, and disulfide reducing agents. Ponticulin is involved in membrane-mediated actin nucleation activity because its removal from detergent-solubilized membranes precludes the reconstitution of this activity (80). However, it is not known whether ponticulin nucleates actin assembly alone or in concert with other membrane components.

Because previous purification schemes generated only small amounts of partially purified ponticulin, very little is known about its physical properties or mechanism of action. The major 17-kD band observed on SDS–polyacrylamide gels has been shown to contain six isoforms (pI 4.1 to 5.3) on two-dimensional gels (16, 104). The amino acid composition of ponticulin purified from plasma membranes by F-actin affinity chromatography and preparative SDS-PAGE suggests that this protein is unusually high in serine (20%), glycine (10%), and alanine (10%) (105). The NH_2-terminal amino acid sequence also has been determined (105). However, essentially nothing is known about the biochemical properties of the native protein.

To characterize ponticulin and its role in nucleating actin assembly, we have developed a rapid and efficient purification procedure, starting with cytoskeletons instead of plasma membranes. We also have determined the hydrodynamic properties of highly purified ponticulin in octylglucoside micelles and have demonstrated that, when reconstituted into *Dictyostelium* lipid vesicles, ponticulin is sufficient for the nucleation of actin assembly. Like actin assembled onto *Dictyostelium* plasma membranes, ponticulin-nucleated actin filaments have both ends free. The hydrodynamic properties and the observed first-order dependence of actin nucleating activity on the protein-to-lipid ratio in reconstituted vesicles indicate that ponticulin behaves as a monomer in both detergent micelles and lipid bilayers. In addition to its previous identification as an actin–membrane anchor, our results suggest that monomeric ponticulin laterally nucleates actin filaments at the plasma membrane during motile processes. These results further suggest that clustering of ponticulin by extracellular factors is not an obligate step in membrane-mediated actin nucleation.

Materials and Methods

Chemicals

All chemicals used were reagent grade unless otherwise specified. Triton X-114 (TX-114), deuterium oxide (D_2O), DTT, 1-ethyl-3-(3-dimethylaminopropyl) carbodiimide, dimyristoyl L-α-phosphatidylcholine (DMPC)[1], and other synthetic phospholipids were purchased from Sigma Chem. Co. (St. Louis, MO). Other cross-linking agents were from Pierce Chem. Co. (Rockford, IL). TX-114 was precondensed three times by the method of Bordier (8). The plasmalogen form of bovine brain phosphatidylethanolamine (PE) was purchased from Avanti Polar Lipids, Inc. (Alabaster, AL). Bio-Beads (SM-2) were purchased from Bio-Rad Laboratories (Richmond, CA). Octylglucoside (OG), phalloidin, and ATP were purchased from Boehringer Mannheim Biochemicals (Indianapolis, IN). *N*-(5-fluoresceinthiocarbamoyl)dipalmitoyl-l-α-phosphatidylethanolamine triethylammonium salt (fluorescein PE) was from Molecular Probes Inc. (Eugene, OR).

Proteins

Actin used for cosedimentation assays and actin affinity columns was isolated from rabbit skeletal muscle according to the method of Spudich and Watt (86). Pyrene actin, used in actin nucleation assays (51), was purified further by gel filtration Sephadex G-150 in 0.2 mM $CaCl_2$, 0.2 mM ATP, 0.5 mM DTT, 2 mM Tris-HCl, pH 8.0 (buffer A; reference 60). Adsorbed R67 IgG, an antibody recognizing ponticulin and two related polypeptides, was prepared as described (16, 103, 104). CapZ was the kind gift of Dr. John A. Cooper, Washington University School of Medicine, St. Louis, MO.

Purification of Ponticulin

Preparation of Cytoskeletons. *D. discoideum* amebas (strain K-AX3 from Dr. Richard Kessin, Columbia University) were grown in HL-5 medium (19) to ~10^7 cells/ml. A total of 4×10^9 cells was used for analytical analyses. 1–1.5 $\times$ 10^{10} cells were used in preparative experiments. All centrifugation steps were carried out at 4°C. Cells were harvested by pelleting for 2 min at 400 *g*, washed twice with 14.6 mM KH_2PO_4, 2.0 mM Na_2HPO_4, pH 6.1, and washed once with 20 mM sodium phosphate, pH 6.8 (PB). Cells were resuspended in PB to 2×10^8 cells/ml and extracted with an equal volume of 2% (vol/vol) TX-114 in 2× cytoskeletal buffer (2× CSK; 20 mM KCl, 20 mM EGTA, 20 mM imidazole, 4 mM $MgCl_2$, pH 7.0) (62). The mixture was incubated for 10 min on ice and then for 10 min at room temperature. Cytoskeletons were recovered as a pellet after centrifugation in a swinging bucket rotor for 4 min at 11,000 *g*.

Isolation of Ponticulin from Cytoskeletons. The cytoskeletal pellet was resuspended to the initial cell suspension volume by homogenization into 2 M NaCl, 1× CSK, 1% TX-114, 1 μM phalloidin. After 30 min of slow rotary mixing at room temperature, the suspension was centrifuged in an SW41 rotor (Beckman Instrs., Inc., Fullerton, CA) at 4°C for 45 min at 28,000 rpm (100,000 *g*). The mixture separated into a buoyant detergent phase, a denser high salt aqueous layer, and a pellet (extracted cytoskeletons). This pellet was reextracted as described above. The two detergent layers were pooled before TX-114 removal.

Removal of TX-114. Bio-Beads were prepared by the method of Holloway (45) and stored in PB. The concentration of TX-114 was determined by reading the OD_{275} of the sample and using the extinction coefficient for the structurally similar TX-100 ($E^{1\%}$ = 21) (45). 1 g of Bio-Beads was sufficient to remove 70 mg of TX-114. The detergent layer was mixed gently with Bio-Beads at 4°C for 30 min. This lowered the TX-114 concentration to ~1%. Immediately after incubation, enough 30% (wt/vol) OG in column buffer (CB; 50 mM KCl, 1 mM $MgCl_2$, 20 mM Tris-acetate, pH 7.0) was added to make the detergent layer 3% OG. This solution was mixed gently at 4°C overnight.

F-Actin Affinity Chromatography. The F-actin affinity matrix was prepared as described (105). A 1-ml column of actin beads was prepared in a 5-ml syringe. The beads were preeluted with 5 ml of 2 M NaCl, 2 mM EGTA, 1% OG, 0.5 μM phalloidin, CB and equilibrated with 10 ml of 1% OG, 1 μM phalloidin, CB. After concentration to ~10 ml with a Centriprep-10 (Amicon, Beverly, MA), the detergent solution containing ponticulin and OG was dialyzed overnight at 4°C against 1% OG, CB. After centrifugation at 100,000 *g* for 30 min, the clarified detergent solution was slowly loaded onto an F-actin column at room temperature or slowly rotated end-over-end with the actin beads in a plastic tube for 1 h at 4°C. Beads and sample were returned to the column and the unbound fraction (run-through) was collected. The beads were washed with 10 ml of 1% OG, 0.5 μM phalloidin, CB and the ponticulin-containing fraction was eluted with 5 ml of 2 M NaCl, 2 mM EGTA, 1% OG, 0.5 μM phalloidin, CB. The beads were reequilibrated, reincubated with the run-through fraction, and eluted as above once or twice more. (With freshly prepared F-actin beads, two incubations and NaCl elutions were sufficient to remove all ponticulin from the run-through; older beads sometimes required a third round.) The NaCl eluates were pooled and concentrated to ~2 ml in a Centricon-10 (Amicon). The concentrated NaCl eluates were dialyzed against 1% OG, CB at 4°C for at least 24 h.

High Pressure Liquid Chromatography Gel Filtration. Ponticulin was gel filtered using two Bio-Sil TSK-125 columns, each 300 × 7.5 mm (Bio-Rad Laboratories), mounted in series on an Ultro Chrom GTi Bioseparation System (Pharmacia LKB Biotechnology, Piscataway, NJ). The system was calibrated with Bio-Rad gel filtration standards. A ponticulin-enriched frac-

1. *Abbreviations used in this paper*: CB, column buffer (50 mM KCl, 1 mM $MgCl_2$, 20 mM Tris-acetate, pH 7.0); DMPC, dimyristoyl L-α-phosphatidylcholine; HIC, hydrophobic interaction chromatography; OG, octylglucoside; PB, 20 mM sodium phosphate buffer, pH 6.8; PC, phosphatidylcholine; PE, phosphatidylethanolamine; TX-114, Triton X-114.

tion (typically 30 μg), obtained by concentration and dialysis of the NaCl-eluted fraction from the actin-affinity matrix, was chromatographed in 1% OG in CB, pH 7.0, at a flow rate of 0.5 ml/min. The volumes of collected fractions were 1.5 ml (fractions 1–5); 0.2 ml (fractions 6–60); and 0.5 ml (fractions 61–75). The total elution volume was 22 ml. The void volume was 10.2 ml.

Hydrophobic Interaction Chromatography (HIC). High pressure HIC was performed at ambient temperature using a TSK Phenyl-5PW column (8 × 75 mm; Pharmacia LKB Biotechnology) equilibrated with 10 column volumes (38 ml) of 0.7% OG, 20 mM Pipes, pH 7.0. A ponticulin-enriched fraction (65 μg in 100 μl), obtained by concentration of the NaCl-eluted fraction from the actin-affinity matrix, was dialyzed extensively at 0–4°C against 1.5% OG, CB. The dialyzed ponticulin was diluted with an equal volume of 20 mM Pipes, pH 7.0, centrifuged through a Spin-X™ filter unit (Costar Corp., Cambridge, MA), and immediately loaded onto the HIC column at a flow rate of 0.1 ml/min. The column was washed with 3.8 ml of 0.7% OG, 20 mM Pipes, pH 7.0, and bound protein was eluted at 0.2 ml/min with 7.6 ml of a gradient of 0.7–1% OG in 20 mM Pipes, pH 7.0. Approximately 60 fractions of 200 μl each were collected. Portions of HIC-purified ponticulin were iodinated with ^{125}I-Bolton-Hunter reagent (New England Nuclear, Boston, MA) in 100 mM sodium phosphate, pH 8.0, to a specific activity of ~3 μCi/μg ponticulin.

SDS-PAGE and Protein Blotting. Samples were denatured at 70°C for 10 min, run on polyacrylamide gradient (10–20%) SDS slab gels using the discontinuous system of Laemmli (53), electrophoretically transferred to nitrocellulose (97), probed with antibody against ponticulin (R67 IgG), and visualized by incubation with ^{125}I–protein A (New England Nuclear) as described previously (16, 104). Prestained molecular mass markers (BRL, Gaithersburg, MD) were lysozyme (15 kD), β-lactoglobulin (18 kD), carbonic anhydrase (29 kD), ovalbumin (46 kD), BSA (69 kD), phosphorylase B (107 kD), and myosin (224 kD). Gels were silver stained according to the method of Merril et al. (63).

Protein Determinations. Protein concentrations were determined in the presence of 1% SDS with the room temperature protocol of the BCA Protein Assay (Pierce Chem. Co.), using BSA as the standard. The amounts of purified ponticulin also were determined by PTC amino acid analyses (31) (see below).

Quantification of Ponticulin

Enrichment during Purification. Various amounts (~0.03 to 90 μg) of whole cells, cytoskeletons, and fractions from the later steps of the purification scheme were analyzed for ponticulin content by immunoblotting as described above. Exposed film was scanned with a densitometer (model 222-020 UltroScan XL; Pharmacia LKB Biotechnology, Inc., or pdi scanning densitometer, Huntington Station, NY), and the areas under the peaks were determined automatically. In some experiments, the autoradiogram was used as a template to excise the ponticulin signal at 17 kD, and the nitrocellulose pieces were counted in a gamma counter. Known amounts of HIC-purified ponticulin were analyzed simultaneously, generating a standard curve from which the amounts of ponticulin in the different fractions were determined. The results from these different methods generally were in close agreement.

Characterization of Purified Ponticulin

Amino Acid Analysis. HIC-purified ponticulin was absorbed to ProBlott™ (polyvinylidene difluoride) membrane pieces (Applied Biosystems, Inc., Foster City, CA) as described (85). Briefly, 100 μl of ponticulin (5.5 μg) containing a trace amount of ^{125}I-ponticulin were diluted into 1.8 ml of sterile filtered PBS (150 mM NaCl, 10 mM sodium phosphate buffer, pH 7.4) in silanized plastic tubes containing pieces of ProBlott™ (previously wetted in 100% methanol followed by several rinses in PBS). After gentle agitation for 24 h at room temperature, the pieces of ProBlott™ were washed seven times with filter-sterilized water. The washed ProBlott™ pieces and recovered PBS solution were counted to determine the percentage of adsorbed ponticulin, and the ProBlott™ pieces were stored at −20°C until analysis. Amino acid compositions of the adsorbed protein were determined using standard techniques (6, 21, 107). Amino acid compositions also were obtained for ponticulin purified by preparative SDS-PAGE and electrotransferred to polyvinylidene difluoride membranes.

Cosedimentation Actin-binding Assays. Actin was polymerized at room temperature by adding 1 vol of 5× polymerization buffer (200 mM KCl, 100 mM Pipes, 10 mM $MgCl_2$, 250 μM $CaCl_2$, pH 7.0) to 4 vol of actin (1–4 mg/ml) in buffer A and stored on ice. 12–18 h before use, the F-actin was dialyzed at 4–6°C against 300–400 vol of 1× polymerization buffer. ^{125}I-Ponticulin was diluted into 1.5% OG in CB and clarified at room temperature in an airfuge (178,000 *g* for 20 min) (Beckman Instrs., Inc.). Each assay (~250 μl final volume) contained 50 μg actin, ~65 ng ^{125}I-ponticulin, 20 μg BSA, ~1% OG, 13 mM Tris, 7 mM Pipes, 50 mM KCl, 2 mM $MgCl_2$, and 50 μM $CaCl_2$, pH 7.0. After a 1-h incubation at room temperature with occasional mixing, the assay mixture was centrifuged at room temperature in an airfuge (178,000 *g* for 20 min; Beckman Instrs., Inc.). The supernatant was collected by aspiration and the pellet was rinsed carefully with 250 μl CB to remove traces of the supernatant. The supernatant, rinse, and pellet were counted, and the supernatant and pellets were analyzed by SDS-PAGE. The rinses generally contained only a few percent of the total counts and were disregarded. Dried gels were exposed to film at −85°C in the presence of an intensifying screen or at room temperature.

Hydrodynamic Properties

Stokes Radius. The Stokes radius of HIC-purified ponticulin was determined at room temperature using both high pressure and conventional gel filtration chromatography. The Bio-Rad gel filtration standards (molecular mass; Stokes radius, R_S) used in the HPLC experiments were bovine IgG (158 kD; 5.1 nm), ovalbumin (43 kD; 2.8 nm), and myoglobin (17 kD; 1.9 nm). Conventional gel filtration chromatography employed a Sephadex G-100 column (17.5 × 0.75 cm) equilibrated with 2% OG in CB. A trace amount of ^{125}I-ponticulin was added as an aid in determining the elution position of ponticulin relative to the following molecular mass standards (molecular mass; Stokes radius, R_S): cytochrome c (12.3 kD; 1.7 nm), myoglobin (17 kD; 1.9 nm), chymotrypsinogen (23.7 kD; 2.2 nm), ovalbumin (43 kD; 2.8 nm), and lactoperoxidase (92.6 kD; 3.6 nm). Column fractions were counted and then analyzed by SDS-PAGE. Most Stokes radii were from Le Maire et al. (54) and Tanford et al. (93); R_S for lactoperoxidase was calculated using a diffusion coefficient (D × 10^7 cm^2 s^{-1}) of 5.95 (84) in the equation, $R_s = kT/6\pi\eta D$ (83).

Sedimentation Coefficient and Partial Specific Volume (ν*). The standard proteins used in sedimentation analyses and the accepted values (84) for their Svedberg coefficients (× 10^{13}) and partial specific volumes (ν^*) were as follows: cytochrome c (1.71 *S*; 0.728 cm^3/g), myoglobin (2.04 *S*; 0.741 cm^3/g), chymotrypsinogen (2.54 *S*; 0.721 cm^3/g), ovalbumin (3.55 *S*; 0.749 cm^3/g), lactoperoxidase (5.37 *S*; 0.764 cm^3/g), and aldolase (7.35 *S*; 0.742 cm^3/g). HIC-purified ponticulin (2 μg) and the standard proteins (10 μg each) were run together on 5–20% sucrose gradients (prepared in 2% OG, CB, and either H_2O or D_2O) at 240,000 *g* for 18 h at 4°C and 25 fractions per gradient (200 μl each) were collected using a density gradient fractionator (model 640; ISCO, Lincoln, NE). Aliquots were analyzed by SDS-PAGE and ponticulin-containing fractions were determined by immunoblotting. The refractive index of each fraction was measured with a Bausch & Lomb refractometer (catalogue No. 33.46.10; Rochester, NY). As the refractive indices appeared to be unaltered by the detergent and buffer used, the percent of sucrose in each fraction and the density of each H_2O-containing fraction were determined from standard tables (73, 100). Densities of D_2O-containing fractions were obtained by linear interpolation between the density of the 5% sucrose (1.122 g/cm^3) and the 20% sucrose (1.168 g/cm^3) (18). Values for average distance sedimented, average density, average viscosity, and $s_{20,w}$ were determined for the standard proteins and ponticulin–OG micelles using the procedure and equations described in Clarke (17) and Clarke and Smigel (18). The molecular weight of the ponticulin–OG micelle was calculated from the equation (83, 91),

$$M = R_S s_{20,w} \left[\frac{6\pi N \eta_{20,H_2O}}{1 + \nu^* \rho_{20,H_2O}} \right],$$

where M = molecular weight, R_s = Stokes radius, $s_{20,w}$ = sedimentation coefficient in pure H_2O at 20°C, N = Avogadro's number, η_{20,H_2O} = the viscosity of water at 20°C (1.002 cp), ν^* = partial specific volume, and ρ_{20,H_2O} = the density of water at 20°C (0.998 g/cm^3). To estimate the asymmetry of the complex, the frictional ratio (f/f_0) for the ponticulin-OG micelle was calculated using the equation (18, 83, 91),

$$\frac{f}{f_0} = R_s \left[\frac{4\pi N}{3M\left(\nu^* + \frac{\delta}{\rho_{20,H_2O}}\right)} \right]^{1/3},$$

where δ = amount of water in g bound per gram of complex (14).

Reconstitution. Ponticulin was reconstituted into vesicles made from *D. discoideum* lipid or various commercially available lipids. *D. discoideum* lipid was extracted from sucrose-Renografin purified plasma membranes

(47), and phospholipid content was estimated from the amount of organic solvent-extractable phosphorus (56). Lipids were dissolved in 1% OG, 20 mM Pipes, pH 7.0, to a final concentration of 1 mM phospholipid, sonicated briefly, and equilibrated for 12–16 h on ice. Lipid solutions then were clarified by centrifugation at room temperature in a Beckman Instrs. Inc. airfuge (178,000 *g* for 20 min) or at 4°C in a Beckman 42.2 Ti rotor (223,000 *g* for 30 min), and mixed with HIC-purified ponticulin in the same buffer. The ponticulin-lipid-detergent mixture (usually ~480-fold molar excess phospholipid over protein) was incubated at room temperature for 4–5 h and then diluted 10–15-fold into buffer. These dilutions lowered the OG concentration far below the critical micelle concentration of ~0.7% (82). Unless stated otherwise, vesicles contained 0.5 μg/ml ponticulin and 14 μM phospholipid. Vesicles containing *D. discoideum* lipid without ponticulin were prepared similarly.

Vesicle Characterization

Electron Microscopy. Vesicles of ponticulin and *D. discoideum* lipid were reconstituted as described above and collected by centrifugation at ~183,000 g_{max} for 3.5 h at 5°C in a Beckman 50Ti rotor. The pellet was resuspended into 2% glutaraldehyde, 0.1 M cacodylate buffer, pH 7.4, and compacted in two Beckman airfuge tubes at ~165,000 g_{max} for 1 h at 20°C. The pellets were washed three times with buffer and postfixed with 2% OsO_4, 0.1 M cacodylate, pH 7.4. After three more washes with buffer, the pellets were stained en bloc with 1% uranyl acetate, 70% ethanol, dehydrated in ethanol, and embedded in Poly/Bed 812 (Polysciences, Inc., Warrington, PA). Silver sections were cut both parallel and perpendicular to the axis of centrifugation with a Diatome diamond knife on a Reichert Ultracut E ultramicrotome. Grids were poststained with 4% uranyl acetate in methanol: 70% ethanol (1:1) for 30 min and with Reynold's lead citrate for 1 min.

Sucrose Gradients. Fluorescein PE (1 μM; 0.1% of the total) and ^{125}I-ponticulin (<25 ng; ~0.2% of the total) were added as tracers to mixtures containing 1% OG, ponticulin, and DMPC or *D. discoideum* lipid (1 mM phospholipid). The mixtures then were diluted 10-fold with 20 mM Pipes, pH 7.0. After collection by centrifugation at 200,000 *g* for 3 h, vesicles (100-μl aliquots) were loaded onto 5–20% sucrose gradients containing 50 mM NaCl, 20 mM Pipes, pH 7.0, and centrifuged in a Beckman SW50.1 rotor (18 h, 45,000 rpm, 4°C). Gradient fractions (200 μl each) were collected with an ISCO density gradient fractionator (model 640) and counted in a gamma counter. 100-μl aliquots of each fraction were diluted into 700 μl of 1% SDS, 50 mM borate, pH 9.0, and their relative fluorescence was measured (λ_{ex} = 495 nm, λ_{em} = 520 nm) in an LS-3 Spectrofluorimeter (Perkin-Elmer Corp., Norwalk, CT). The refractive indices of peak fractions also were determined.

Pyrene-Actin Assays

Actin Nucleation. Reconstituted ponticulin vesicles and control vesicles were assayed for actin nucleation activity using the pyrene-actin fluorescence assay (23, 80). Vesicles, without fluorescein PE or radiolabel, were prepared in assay buffer (25 mM imidazole, 100 mM KCl, 2 mM $MgCl_2$, 100 μM $CaCl_2$, 100 μM ATP, pH 7.0, final concentrations). The final concentration of OG in the assays was <0.1%. In some experiments, CapZ (60 nM) was premixed with ponticulin (30 nM) in *Dictyostelium* lipid vesicles (14.4 μM phospholipid) before addition of actin. Controls showed that about half the CapZ was inactivated by binding to *Dictyostelium* lipid under these conditions. Actin (10% pyrene-labeled; 3 μM final concentration) was added to samples in assay buffer, and the initial changes in pyrene-actin fluorescence were monitored (λ_{ex} = 365 nm; λ_{em} = 407 nm). Background fluorescence was subtracted and the corrected numbers were normalized between 0 and 10, with 10 denoting the fluorescence after 24 h of polymerization. Nucleation activity was estimated from the maximal rate of fluorescence increase observed during the first 15 min after initiation of polymerization (80).

Actin Depolymerization. For depolymerization experiments, portions of pyrene-labeled actin (5.0 μM, 20% pyrene-labeled) were polymerized in the presence or absence of ponticulin (~60 nM) in *Dictyostelium* lipid vesicles (~30 μM phospholipid). After 2 h at 24°C, CapZ was added to a final concentration of 60 nM in half the samples, and incubation at 24°C was continued for another 24 h. Initial rates of actin depolymerization were measured by diluting samples 10-fold into a cuvette containing assay buffer and monitoring changes in pyrene fluorescence. Under these conditions, depolymerization should occur only from the pointed ends of the actin filaments (72). As controls, aliquots also were diluted into assay buffer containing 5 μM phalloidin. Fluorescence was normalized from 0 to 100%, with 100% denoting the fluorescence of each sample at the earliest measurable time point.

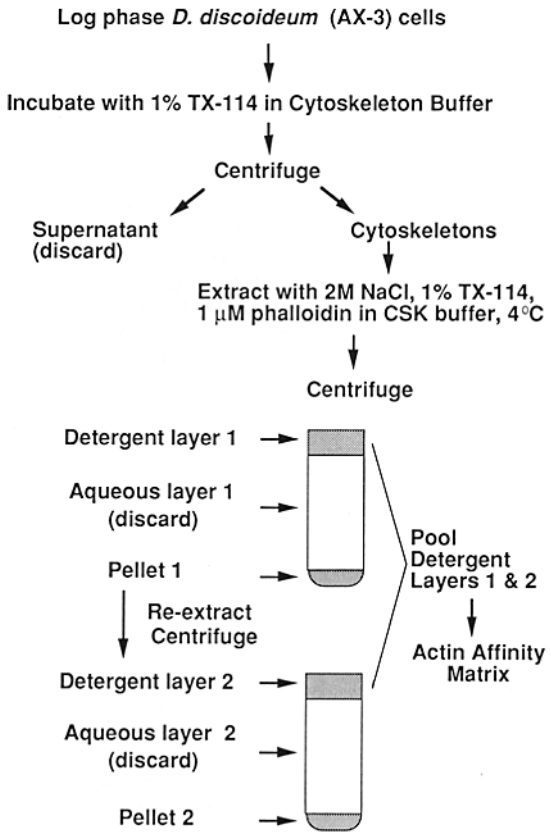

Figure 1. Procedure for the extraction of ponticulin from *Dictyostelium* cytoskeletons. Ponticulin-enriched fractions are shaded. Note that, unlike a typical TX-114 phase separation in which the detergent forms the lower phase, the detergent layer is less dense than 2 M NaCl.

Results

Purification

Ponticulin, an F-actin binding plasma membrane glycoprotein (16, 103) also is a component of the cytoskeleton (104). When log-phase *D. discoideum* amebas were extracted with 1% Triton X-100 in CSK buffer, 92.6 ± 4.0% (n = 3) of the ponticulin, as detected on immunoblots, pelleted with the cytoskeletons (data not shown). Trace amounts of 15- and 19-kD polypeptides, proteins that may be structurally related to ponticulin (104), also were observed in these Triton-insoluble residues.

We developed a protocol for the rapid purification of ponticulin that takes advantage of its cytoskeletal association, hydrophobic nature, and salt-sensitive binding to F-actin (103). The initial steps of this procedure are outlined in Fig. 1 (see also Materials and Methods). First, cytoskeletons are prepared by extracting whole cells with a cytoskeleton-stabilizing buffer containing TX-114. Solutions containing this detergent spontaneously form a TX-114–enriched hydrophobic phase and a TX-114–depleted aqueous phase when heated above 20°C, the cloud point of the detergent (38). The

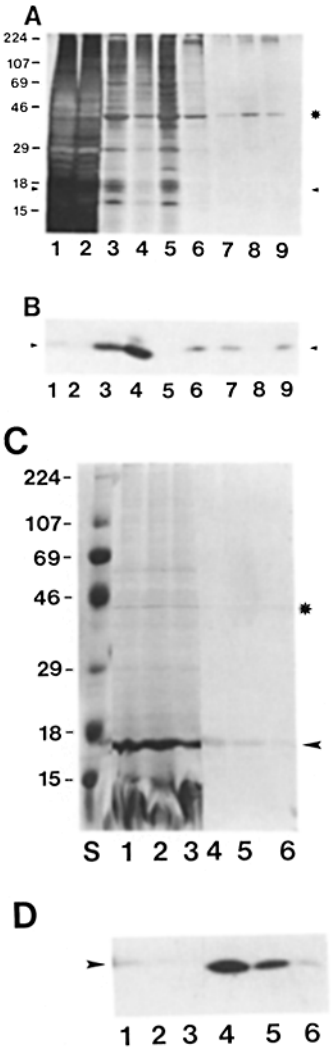

Figure 2. Ponticulin partitions into the hydrophobic detergent (TX-114) phase after salt-induced dissociation from cytoskeletons and is the major hydrophobic protein eluted by 2 M NaCl from F-actin columns. Silver-stained gel (*A*) and autoradiogram of the 15–20-kD region of a protein blot probed with adsorbed R67 IgG followed by ^{125}I-protein A (*B*) of fractions from an analytical preparation. Lane *1*, whole cells; lane *2*, cytoskeletal supernatant; lane *3*, cytoskeletal pellet; lane *4*, detergent layer 1; lane *5*, aqueous layer 1; lane *6*, pellet 1; lane *7*, detergent layer 2; lane *8*, aqueous layer 2; and lane *9*, pellet 2. All fractions were resuspended to the original volume of suspended cells (20 ml, ~9 mg/ ml). 20 μl of each fraction was loaded onto the gel. Because of overloading of the gel, ponticulin is underrepresented in lanes *1–3* of *B*. Film was exposed for 88 h at −85°C. Silver-stained gel (*C*) and autoradiogram of the 15–20-kD region of an antiponticulin immunoblot (*D*) showing the protein and ponticulin content of fractions from an F-actin affinity column. Lane *S*, molecular mass standards. Lanes *1–3*, run-through fractions (20 μl) from three consecutive passages of the detergent layer through the F-actin column; and lanes *4–6*, the corresponding salt-eluted fractions (20 μl) from the F-actin column. Film was exposed for 12 h at −85°C. Molecular mass standards, in kD, are shown on the left. Asterisks in *A* and *C* indicate the position of actin; arrowheads indicate the position of ponticulin.

temperature at which phase separation occurs is lowered even further by increasing the salt concentration of the initial solution (30, 69). Proteins such as ponticulin, that are bound by electrostatic interactions to the cytoskeleton, can be dissociated with 2 M NaCl in buffer containing TX-114. Subsequent phase separation at 4°C generates a detergent-rich phase containing hydrophobic proteins that bind to cytoskeletons at physiological, but not at high, concentrations of salt. Because variable amounts of ponticulin remain associated with the cytoskeletal pellet after the first extraction, the pellet is reextracted with 2 M NaCl and TX-114.

As expected, ponticulin was greatly enriched in the detergent layers generated by this procedure (Fig. 2). A 43-kD polypeptide, probably actin, was prominent in the whole cell extract (Fig. 2 *A*, lane *1*), relatively depleted in the initial TX-114 supernatant (Fig. 2 *A*, lane *2*) and enriched in the TX-114–insoluble cytoskeletons (Fig. 2 *A*, lane *3*). The TX-114 cytoskeletons also contained ~85% of the total cellular ponticulin (Table I; Fig. 2 *B*, lane *3*). After phase separation, most of the cytoskeletal ponticulin usually was recovered in the first detergent layer (Fig. 2, *A* and *B*, lanes *4*). However, appreciable amounts (sometimes most) of the ponticulin continued to pellet with the cytoskeletons (Fig. 2, *A* and *B*, lanes *6*). Therefore, the cytoskeletal pellet was reextracted with 2 M NaCl and 1% TX-114, and additional ponticulin was recovered in the second detergent layer (Fig. 2, *A* and *B*, lanes *7*). Very little ponticulin was found in either aqueous layer (Fig. 2, *A* and *B*, lanes *5* and *8*), confirming the hydrophobic nature of this protein. Even with the difficulty of cleanly separating the detergent and aqueous layers, ponticulin was enriched ~58-fold in the combined detergent layers compared with the whole cell extract (Table I). The detergent layers were pooled and most of the TX-114 was exchanged with OG before F-actin affinity chromatography.

As much as one third of the cellular ponticulin always remained tightly bound to the cytoskeletons and was discarded (Fig. 2, *A* and *B*, lanes *9*). Only two high salt extractions usually were performed because resuspension of the cytoskeletal pellets was difficult after repeated ultracentrifugations. Extractions with 4 M NaCl resulted in higher initial yields of ponticulin but the additional ponticulin aggregated irreversibly and final recovery was lower.

*Table I. Purification of Ponticulin**

Step	Volume	Protein‡ (in 10^{10} cells)	Ponticulin§ (in 10^{10} cells)	% Ponticulin of total protein	Step-fold purification	Total fold purification	Recovery
	ml	*mg*	*mg*				%
Cells	69	505	0.33	0.065	1.0	1.0	100
Cytoskeletons	69	48.5	0.28	0.58	8.9	8.9	85
Pooled detergent layers	19	4.68	0.18	3.8	6.6	58	54
Concentrated NaCl eluate	1.2	0.12	0.090	75	19.7	1150	27
HIC	1.2	0.084	0.084	>99	1.32	1523	25
Gel Filtration	1.5	0.066	0.066	>98	1.30	1508	20

* Data from a single analytical experiment. In replicate experiments, ponticulin was estimated to comprise 0.040% and 0.047% of the total cell protein, and the fold purification of the final, highly purified ponticulin was proportionately higher.
‡ Determined by BCA assay and normalized to 10^{10} cells.
§ Determined by autoradiography and normalized to 10^{10} cells. Values for ponticulin in cells and cytoskeletons may be underestimates because the total signal at 17 kD increased during purification. Other 17-kD protein(s) in these crude fractions apparently interfered with the detection of ponticulin on immunoblots, especially at high protein loads (Fig. 2).

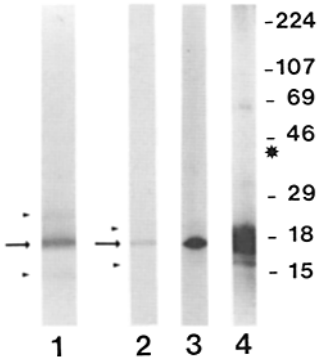

Figure 3. Highly purified ponticulin is obtained by gel-filtration or HIC of the pooled salt eluates from the F-actin affinity column. Lanes from silver-stained SDS-gels showing peak fractions of ponticulin after either HPLC gel-filtration (lane *1*) or HIC (lane *2*). As a further test of purity, the material in lane *2* was radioiodinated and analyzed by SDS-PAGE and autoradiography at room temperature (lanes *3* and *4*). Small amounts of 15-kD and 19-kD polypeptides (*arrowheads*) copurify with ponticulin (*arrows*), but no actin (*) is detectable, even after prolonged exposure to film (lane *4*). The positions of molecular mass standards, in kD are indicated on the right. Lane *3*, ~2,700 cpm of ^{125}Iponticulin exposed to film for 23 h; and lane *4*, ~210,000 cpm exposed for 15 h.

Ponticulin was separated from most other proteins in the pooled detergent layers by F-actin affinity chromatography. As observed with detergent-solubilized *D. discoideum* plasma membranes (103), a major 17-kD polypeptide in the detergent layers bound F-actin columns under physiological buffer conditions and was eluted with high salt (Fig. 2 *C*, lanes *4–6*). Minor amounts of other proteins, including actin and 15-kD and 19-kD polypeptides, also eluted under these conditions. Immunoblotting with adsorbed R67 antibody identified the 17-kD polypeptide as ponticulin (Fig. 2 *D*). Essentially all of the ponticulin in the detergent layers was recovered after two or three successive passages through the F-actin column (Fig. 2 *D*, lanes *1–3*). Ponticulin was enriched nearly 20-fold in the salt-eluted fractions relative to the pooled detergent layers (Table I).

Ponticulin was further purified by either gel filtration or hydrophobic interaction chromatography (Fig. 3). Because ponticulin has essentially no absorbance at 280 nm, fractions containing ponticulin were identified using SDS-PAGE. Both gel filtration and HIC yielded fractions containing a major 17-kD protein and minor 15-kD and 19-kD polypeptides (Fig. 3, lanes *1* and *2*). The 17-kD polypeptide was identified as ponticulin by immunoblotting with absorbed R67 IgG (data not shown).

HIC was more efficient than gel filtration chromatography as a final purification step. Almost 93% of the initial ponticulin load was recovered after HIC in contrast to an 80% recovery after gel filtration (Table I). Based on the recovery of 84 μg of ponticulin per 10^{10} cells, as determined from amino acid analyses, a 1,520-fold purification of ponticulin was achieved. This degree of purification was slightly larger than the 1,508-fold purification calculated for gel-filtered ponticulin (Table I).

The purity of HIC-purified ponticulin (Fig. 3, lane *2*) was examined by radioiodination followed by SDS-PAGE and autoradiography (Fig. 3, lanes *3* and *4*). Although a number of minor contaminating proteins could be detected by this method, even overexposed films showed no signal at the position of actin (Fig. 3, lane *4*).

As another test of purity, we compared the amino acid composition of HIC-purified ponticulin (Fig. 3, lanes *2–4*) with the amino acid composition of ponticulin purified by preparative SDS-PAGE followed by electrotransfer to PVDF membranes (Table II); (105). The amino acid compositions obtained for ponticulin purified by these different methods were very similar (Table II). Ponticulin contains relatively large amounts of serine (17–20 mol %), asparagine + aspartate (10–12 mol %), alanine (~10 mol %), threonine (~9 mol %), and glycine (7–9 mol %). It has little or no methionine or histidine. Ponticulin's weak absorbance at 280 nm indicates that it probably does not contain tryptophan, which could not be measured after acid hydrolysis. Based on the amino acid composition (20), the partial specific volume, v^*, of ponticulin was predicted to be 0.716 cm^3/g (the inverse of a density of 1.40 g/ml), which is close to the average v^* observed for a wide range of proteins (14). This predicted value for v^* should be considered an upper estimate because oligosaccharides, known to be present on ponticulin (16, 103), may reduce v^* to 0.68–0.70 cm^3/g (37, 79).

Table II. Amino Acid Analysis of HIC- and SDS-purified Ponticulin

Amino acid	HIC-Purified ponticulin*	SDS-PAGE purified ponticulin*	Residues per polypeptide‖
	mol %	*mol %*	*n*
Asx	11.7 ± 0.5	10.4 ± 1.1	17
Glx	7.8 ± 0.2	5.8 ± 0.3	10
Ser	17.2 ± 0.6	19.8 ± 1.0	32
Gly	6.9 ± 0.6	9.0 ± 1.9	15
His	0.5 ± 0.1	0.4 ± 0.8	1 ± 1
Arg	1.7 ± 0.4	1.5 ± 1.4	2 ± 2
Thr	9.0 ± 0.7	9.3 ± 0.6	15
Ala	9.5 ± 0.8	10.0 ± 0.8	16
Pro	4.0 ± 0.3	3.6 ± 0.5	6
Tyr	2.5 ± 0.6	2.8 ± 0.4	5
Val	6.2 ± 0.3	5.2 ± 0.4	8
Met	0.9 ± 0.4	0.7 ± 0.5	1
Cys	ND‡	4.4 ± 1.1§	7§
Ile	4.7 ± 0.1	4.4 ± 0.7	7
Leu	7.6 ± 0.3	6.7 ± 0.7	11
Phe	4.5 ± 0.2	4.0 ± 0.4	7
Lys	5.2 ± 0.4	4.0 ± 0.2	7
Trp	ND‡	ND‡	ND‡
			167 residues

* Average of four determinations with standard deviations.
‡ Not determined.
§ Average of two determinations; error indicates measurement range.
‖ Based on molecular mass = 16,970 (as determined by SDS-PAGE).

Amino acid analyses also were used to assess the accuracy of the BCA protein assay for ponticulin. Trace amounts of ^{125}I-ponticulin were used to monitor the adsorption of the protein to the polyvinylidene difluoride membrane. Because 93.8 ± 1.8% (n = 4) of the radiolabeled protein was adsorbed and retained on the membranes through multiple washes, we assumed that ~94% of the unlabeled protein mass also was retained. A comparison of the amino acid analyses with the BCA assay results indicated that the BCA assay overestimated by a factor of two the protein concentration of highly purified ponticulin. Calculations for the concentrated NaCl eluate, HIC, and gel-filtered ponticulin take into account this twofold overestimate (Table I).

Characterization of Purified Ponticulin

HIC-purified ponticulin retained the ability to bind F-actin (Fig. 4). In sedimentation assays, at least 74% of freshly

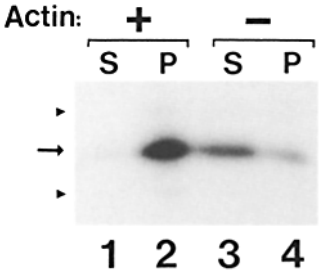

Figure 4. HIC-purified ponticulin binds F-actin. Supernatants (*S*) and pellets (*P*) from sedimentation assays containing ~15 nM ^{125}I-ponticulin with (lanes *1* and *2*) and without (lanes *3* and *4*) 4.6 μM F-actin. Samples were analyzed by SDS-PAGE and autoradiography. Arrow indicates the position of ponticulin; arrowheads indicate the positions of the 15- and 19-kD polypeptides. Film was exposed for 24 h.

purified, OG-solubilized ^{125}I-ponticulin pelleted with F-actin (Fig. 4, lane *2*). By contrast, only 18 ± 6% (n = 4) of the counts sedimented in the absence of F-actin (Fig. 4, lane *4*). Therefore, at least half of the ponticulin appeared to specifically associate with actin. Unbound ponticulin may be in equilibrium with ponticulin bound to actin because OG-solubilized ponticulin in initial run-through fractions from F-actin columns bound actin in subsequent passages through this column (Fig. 2 *D*, lanes *1–3*). If this is true, the dissociation constant for the ponticulin–actin interaction is ~5 μM. However, the stochastic aggregation of the ^{125}I-ponticulin during these assays (Fig. 4, lane *4*) confounded a precise determination of this value.

To determine the likely size and shape of ponticulin–detergent complexes, estimates of the partial specific volume (v^*) and the sedimentation coefficient ($s_{20,w}$) were derived from the sedimentation behavior of these complexes in sucrose density gradients prepared with H_2O and D_2O (17, 18) (Table III). Like other detergent-solubilized integral membrane proteins (17, 42, 70), ponticulin in OG micelles exhibited a lower apparent sedimentation coefficient in D_2O than in H_2O (Fig. 5 *A*). HIC-purified ponticulin exhibited an apparent sedimentation coefficient of 2.5 ± 0.2 *S* (n = 4) in H_2O gradients, while the apparent sedimentation coefficient was only 1.4 ± 0.3 *S* (n = 2) in D_2O gradients. This difference in apparent sedimentation rate indicates that the ponticulin–OG micelle has a larger v^* than those of the soluble protein standards which average 0.74 ± 0.02 cm³/g (see Materials and Methods). Specifically, v^* for the ponticulin–OG micelle was calculated to be 0.825 ± 0.015 cm³/g

*Table III. Hydrodynamic Properties of the Ponticulin-OG Micelle**

Property	Value
Sedimentation coefficient, $S_{20,w}$ ($\times 10^{13}$ s)‡	2.42 ± 0.05
Partial specific volume, v^* (cm³/g)‡	0.825 ± 0.015
Stokes radius, R_s (nm)§	3.6 ± 0.3 (n = 5)
Stokes radius, R_s (nm)‖	3.5 ± 0.4 (n = 2)
Molecular mass (kD)¶	56 ± 6
Detergent bound (g OG/g protein)	2.3 ± 0.4
Frictional ratio, f/f_o**	
0.2 g H_2O/g (minimum estimate)	1.26
1.4 g H_2O/g (maximum estimate)	0.98

* 2% OG.
‡ Determined by the method of Clarke and Smigel (18).
§ Determined by HPLC gel filtration.
‖ Determined by conventional gel filtration chromatography.
¶ Calculated using R_s = 3.6 nm, $S_{20,w}$ = 2.42 *S*, and v^* = 0.825 cm³/g.
** Calculated using R_s = 3.6 nm, M = 56 kD, and v^* = 0.825 cm³/g.

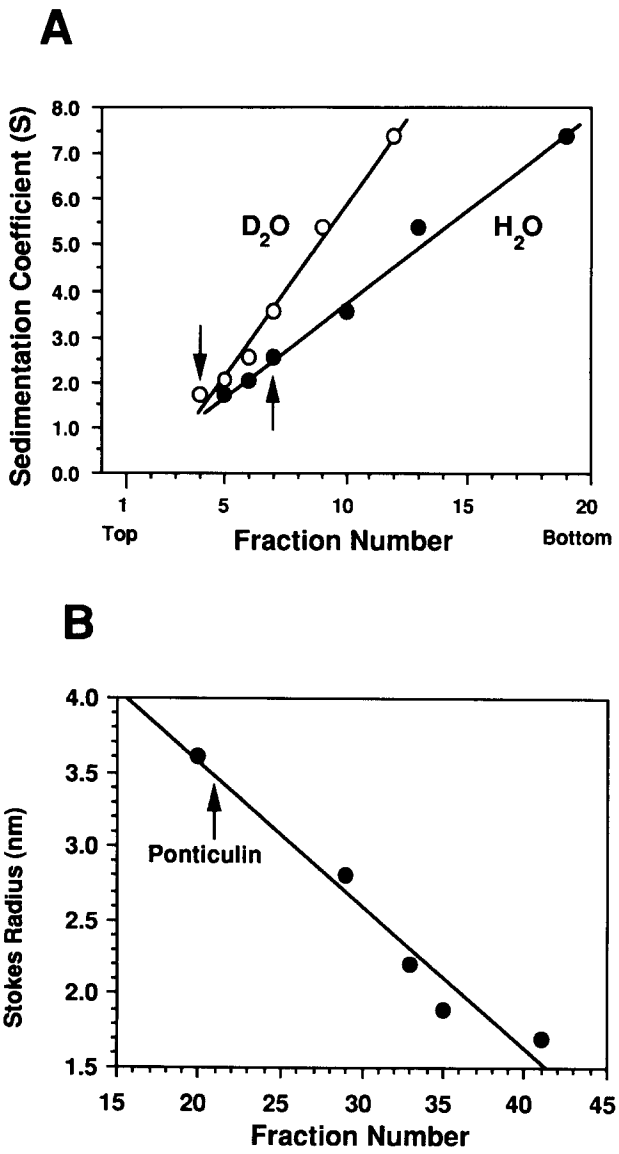

Figure 5. Physical properties of the ponticulin-octylglucoside micelle. (*A*) Sedimentation in sucrose density gradients (5–20%). The apparent sedimentation coefficient of HIC-purified ponticulin in 2% OG, H_2O (●) is 2.5 ± 0.2 *S* (n = 4). In gradients prepared in D_2O (○), the apparent sedimentation coefficient is 1.4 ± 0.3 *S* (n = 2). Arrows indicate position of ponticulin. (*B*) Chromatography on Sephadex G-100. The Stokes radius (R_s) of HIC-purified ponticulin in 2% OG is ~3.6 nm (see text). Arrow indicates elution position of ponticulin.

(theoretically equivalent to a density of ~1.21 g/cm³), a value larger than that (~0.716 cm³/g) predicted from amino acid analyses of the protein alone, but comparable to values (0.82–0.84 cm³/g) obtained for other integral membrane proteins in detergent micelles (14, 24, 30, 39, 67). Using the calculated value for v^* to convert the apparent sedimentation coefficients to standard conditions (H_2O at 20°C) (17, 18), we obtained a value of 2.42 ± 0.05 *S* for the ponticulin–OG micelle (Table III).

The Stokes radius of ponticulin in OG micelles was determined by gel filtration chromatography under both high pressure and normal atmospheric conditions. From the HPLC gel filtration experiments (not shown), a Stokes ra-

dius, R_s, of 3.6 ± 0.3 nm (n = 5) was calculated using the method of Nalecz et al. (66). This value was confirmed by conventional chromatography on a Sephadex G-100 column, which yielded a Stokes radius of 3.5 ± 0.4 nm (n = 2) (Fig. 5 *B*).

Using the values R_s = 3.6 nm, s = 2.42 S, and v^* = 0.825 cm³/g, we calculate a molecular mass of 56 ± 6 kD for the ponticulin–OG micelle. This size and v^* are those expected for a ponticulin monomer of 13–17 kD in an OG micelle of 30–40 kD, the approximate size reported for pure OG micelles in sedimentation velocity experiments (55). The relatively large v^* for the complex, which is not far from the reported v^* for OG (0.859 cm³/g) (75), is inconsistent with the presence of ponticulin dimers or oligomers in OG micelles. For instance, a 26-kD ponticulin dimer in a micelle with 30-kD of OG should exhibit a v^* of [26/56(0.716) + 30/56(0.859)] = 0.792, a number well outside the experimental range. Thus, the micellar detergent-to-protein mass ratio appears to be at least 2.3 mg OG per mg ponticulin. The presence of residual TX-114 is contraindicated by the absence of a detectable absorbance at 280 nm, but the presence of tightly associated endogenous lipid cannot be excluded.

Although tightly bound lipid also would increase v^*, its possible presence should not affect the conclusion that ponticulin is monomeric in OG micelles. To account for our experimental values, ~66% of the OG in a dimer-containing micelle would have to be replaced by endogenous phospholipid (average v^* ~0.95 cm³/g) (61). This eventuality is highly unlikely because OG–phospholipid mixed micelles are stable only when OG is present in a 3.2-fold molar excess (2).

The calculated frictional ratio, f/f_o, for a 56-kD ponticulin–OG micelle is 1.26, assuming a hydration factor (δ) of 0.2 g H_2O/g micelle, a minimum estimate often used for soluble proteins (14, 27, 91). A particle with this frictional coefficient is ellipsoidal with an axial ratio of about 5 (12, 24). However, δ for a protein–detergent micelle may be much larger (18). For instance, a maximum hydration factor of 1.4 g H_2O/g has been reported for Triton X-100 micelles (106). If this higher estimate is used, f/f_o = 0.98, indicating an essentially spherical protein–detergent micelle.

Reconstitution of Bilayer Structure

Ponticulin was readily incorporated into lipid bilayers made either with lipids extracted from *Dictyostelium* plasma membranes or with the synthetic lipid DMPC (Fig. 6). However, the efficiency of incorporation was higher with *Dictyostelium* lipid. About 66% of ^{125}I-labeled ponticulin cosedimented with *Dictyostelium* lipid (Fig. 6 *A*, fractions 4–10), compared with ~28% of ponticulin reconstituted with DMPC (Fig. 6 *B*, fractions 14–19). This behavior contrasted with that of the lipid tracer, fluorescein-PE, which incorporated more efficiently into DMPC vesicles. When reconstituted with *Dictyostelium* lipid (Fig. 6 *A*), ^{125}I-labeled ponticulin sedimented a shorter distance into the sucrose gradient than after reconstitution into DMPC (Fig 6 *B*), but further than ponticulin diluted in the absence of lipid (*P*, Fig. 6 *A*), indicating that the protein's final position in the gradient depended upon association with lipid. The lipid-dependent differences in sedimentability might be due to intrinsic differences in vesicle density (apparent density of 1.031 g/cm³ for ponticulin/*Dictyostelium* lipid, compared to 1.050 g/cm³ for ponticulin/DMPC), but also may reflect a greater degree of resealing for vesicles containing *Dictyostelium* lipid (39, 87).

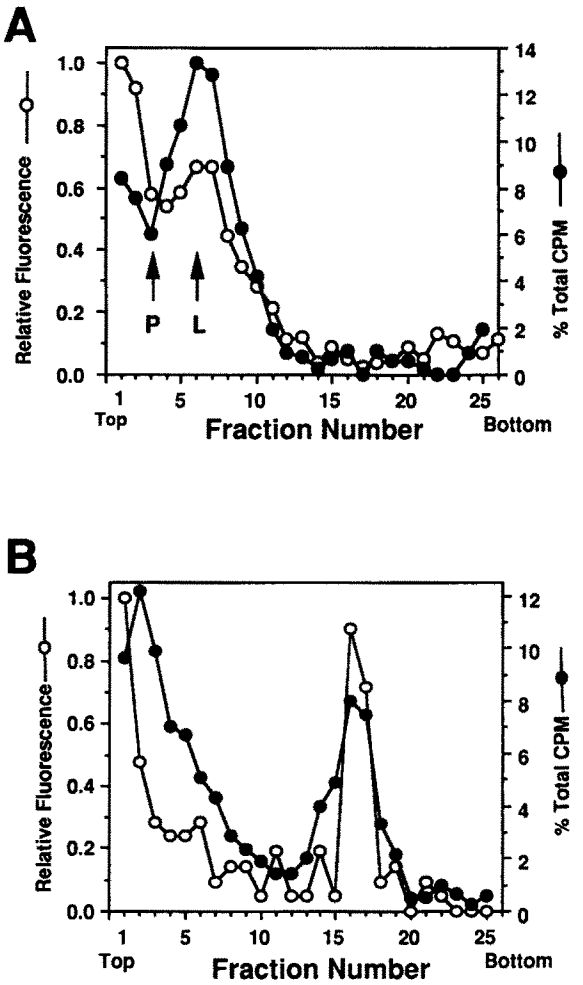

Figure 6. Ponticulin cosediments with lipid vesicles. Vesicles containing HIC-purified ponticulin were prepared by dilution using either *Dictyostelium* lipids (*A*) or DMPC (*B*). ^{125}I-labeled ponticulin (●) and fluorescein-labeled PE (○) were included as tracers. The sedimentation positions of ponticulin in the absence of lipid (*P*) and of *Dictyostelium* lipid vesicles in the absence of ponticulin (*L*) are indicated by arrows. Presumably, the low sedimentability of ponticulin alone (*P*) is due to the small amount (0.1 μg) used for this experiment and the rapidity of the dilution, because higher concentrations of ponticulin aggregated irreversibly and precipitated in the absence of detergent or lipid (not shown).

Reconstituted mixtures of ponticulin and *Dictyostelium* lipid formed vesicles and membrane sheets with ~6-nm-wide trilaminar bilayers (Fig. 7). Apparent vesicle diameters varied from ~80 nm to ~4 μm, with most between ~0.2 and ~0.5 μm. No amorphous material indicative of denatured protein was seen. The electron densities of the outer leaflets of the trilaminar bilayers were variable (Fig. 7, *inset*), perhaps reflecting local differences in lipid or amounts of incorporated protein, possibly induced by glutaraldehyde treatment.

Actin Nucleation Activity

HIC-purified ponticulin reconstituted into *Dictyostelium*

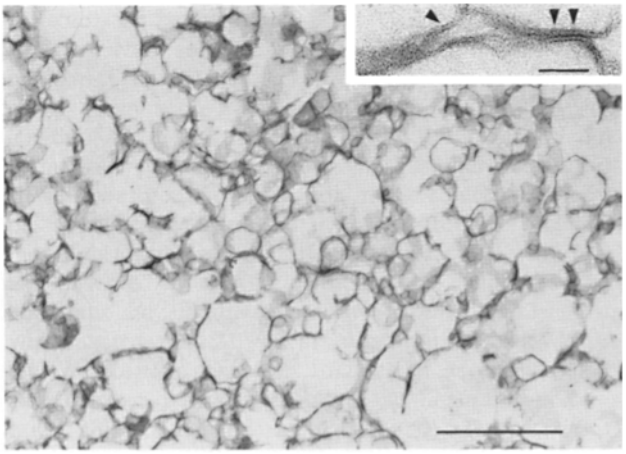

Figure 7. Vesicles and membrane sheets form after dilution of ponticulin-lipid-OG mixtures. These structures are from the upper half of a transverse section through a high-speed pellet of ponticulin reconstituted into *Dictyostelium* lipid. Bar, 1.0 μm. (*Inset*) Variability in appearance of the trilaminar bilayers. Most bilayer profiles contained relatively little electron density (*arrowhead*), but some areas, particularly those at points of contact between the glutaraldehyde-cross-linked vesicles, were considerably more osmophilic (*double arrowheads*). Bar, 50 nm.

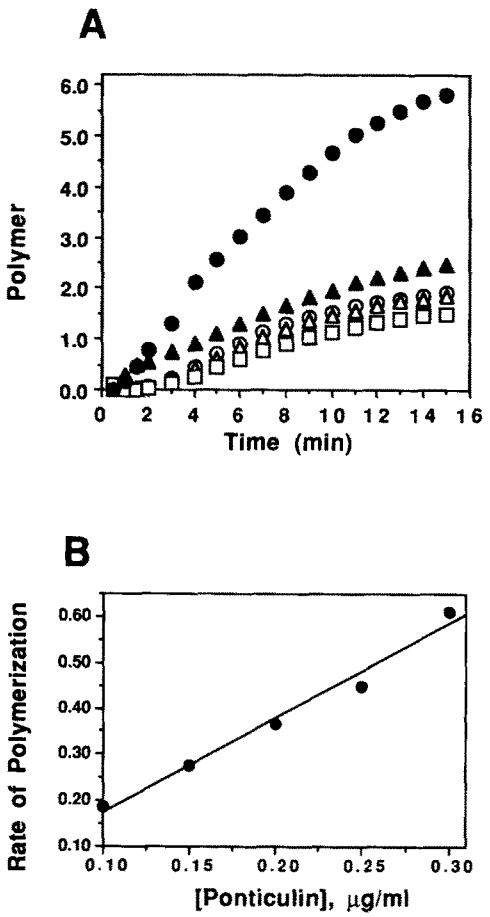

Figure 8. Ponticulin reconstituted into *Dictyostelium* lipid bilayers nucleates actin filament assembly. (*A*) Polymerization kinetics as a function of vesicle composition. HIC-purified ponticulin and various lipids or lipid mixtures were reconstituted by detergent dilution and tested for nucleation activity as described in Materials and Methods. Actin and ponticulin reconstituted into vesicles with lipid from *Dictyostelium* plasma membranes (●); actin and ponticulin reconstituted with DMPC (▲); actin and ponticulin without lipids (△); actin only (○); and actin and *Dictyostelium* lipid vesicles without ponticulin (□). (*B*) Maximal rates of polymerization (from the slopes of curves such as those shown in *A*) versus increasing amounts of ponticulin in *Dictyostelium* lipid vesicles (ponticulin-to-lipid mole ratio = 1:480). The slope of the line shown is 2.04 min^{-1} $(\mu g/ml)^{-1}$ and the correlation coefficient (R^2) is 0.978. Slopes obtained in other experiments were 1.51, 1.64, 1.33, and 0.74 min^{-1} $(\mu g/ml)^{-1}$.

lipid vesicles promoted the assembly of pyrene-labeled actin in nucleation assays (Fig. 8). The shapes of the polymerization time courses were similar to those reported previously for *Dictyostelium* plasma membranes (80), with the maximal polymerization rate observed after a short lag. In agreement with previous observations (16, 80), ponticulin-mediated actin nucleation activity required both the presence of ponticulin and its incorporation into a lipid bilayer (Fig. 8 *A*). Neither *Dictyostelium* lipid vesicles without ponticulin nor ponticulin diluted in the absence of lipid promoted actin filament assembly.

Ponticulin-mediated actin nucleation activity depended critically on the composition of the lipid bilayer. Ponticulin reconstituted into vesicles composed of either DMPC (Fig. 8 *A*) or several other commercially available lipids and lipid mixtures (not shown) exhibited <11% of the nucleation activity observed for ponticulin in *Dictyostelium* lipid vesicles. Even after correcting for the lower incorporation efficiency (Fig. 6), the nucleation activity of ponticulin/DMPC vesicles is ⩽ 26% of that observed for ponticulin in *Dictyostelium* lipid. The critical factor appeared not to be bilayer fluidity per se because neither phosphatidylcholines (PCs) with low gel-fluid chain melting temperatures (T_c's), such as dioleoyl-L-α-PC (T_c = −21°C) and egg PC (T_c = −15 to −5°C), nor relatively high-melting PCs, such as DMPC (T_c = 23.5°C) and dipalmitoyl-L-α-PC (T_c = 41.5°C), supported ponticulin-mediated actin nucleation. Also, neither the bilayer curvature nor the elastic stress (40, 41) attributed to hexagonal-phase phospholipids (25) was the sole critical factor since ponticulin-mediated actin nucleation activity was not supported by PEs with low lamellar-to-hexagonal phase transitions (T_H's), such as dioleoyl-L-α-PE (T_c = −16°C, T_H = 12°C) and the plasmalogen form of bovine brain PE (T_c = 3°C, T_H = 18°C). (T_c and T_H values are taken from references 7, 52, 61.) In addition, no activity was observed with an equimolar mixture of dioleoyl-L-α-PC, dioleoyl-L-α-PE, and bovine brain plasmalogen PE, a composition that approximates that of the three most prevalent phospholipids, ~84% of the total (101), in the *Dictyostelium* plasma membrane. Finally, 1,2-dioctanoyl-*sn*-glycerol (1.0 μM), a lipid recently shown to increase the actin nucleation activity of isolated *Dictyostelium* plasma membranes (81), did not affect the nucleation activity of ponticulin in DMPC bilayers. This result is consistent with the previous conclusion that diacylglycerols act through a tightly bound peripheral protein, rather than directly with ponticulin (81).

Essentially all of the basal actin nucleation activity of *Dictyostelium* plasma membranes appears to be attributable to ponticulin. First, the maximal rate of actin polymerization as a function of the concentration of ponticulin in *Dictyostelium* lipid vesicles is 1.45 ± 0.48 min^{-1} (μg/ml pro-

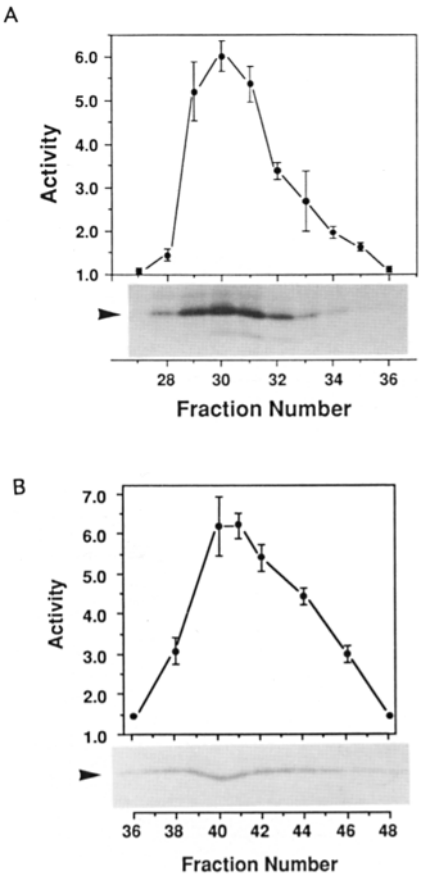

Figure 9. Ponticulin and actin nucleation activity copurify. Ponticulin-containing fractions from gel filtration columns (*A*) or HIC (*B*) were reconstituted with *Dictyostelium* lipid and assayed for actin nucleation activity. Activity is shown above the 12–22-kD region of a silver-stained SDS gel loaded with 40 μl (*A*) or 10 μl (*B*) of each fraction. (*A*) 40 μl of each fraction was premixed with 7 μl of OG-solubilized *Dictyostelium* plasma membrane lipids (7 nmol phospholipid) and reconstituted into vesicles by an 11-fold dilution into assay buffer. (*B*) 30 μl of each fraction was premixed with 7 μl of OG-solubilized *Dictyostelium* lipids (7 nmol phospholipid) and reconstituted into vesicles by a 13-fold dilution. Peaks of activity are coincident with the peaks of ponticulin. Fractions without ponticulin (not shown) exhibited no activity above that of actin alone, which was normalized to 1.0. Error bars indicate the standard deviation of replicate assays (n = 3).

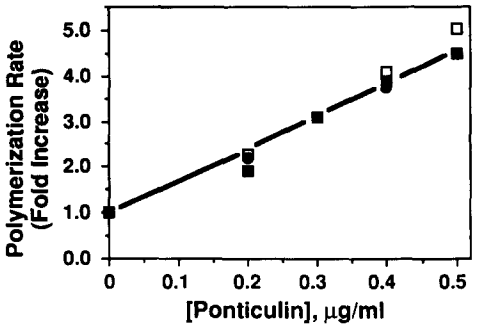

Figure 10. Nucleation activity is relatively independent of the ponticulin-to-lipid ratio. Fold increases in nucleation activity as a function of ponticulin concentration were obtained from curves such as those shown in Fig. 8 *A*. Ponticulin was reconstituted into vesicles such that the final concentration of *Dictyostelium* lipid was (■) 1.4 μM, (□) 14 μM, or (●) 70 μM in the assay mixture. The fold increase in actin nucleation activity was obtained by dividing the maximal rate of actin polymerization of each time course by the maximal rate of polymerization observed for actin alone (80, 81).

tein)$^{-1}$ (n = 5) (Fig. 8 *B*). The comparable rate for *Dictyostelium* plasma membranes in the absence of exogenous diacylglycerol is ~0.013 min^{-1} (μg/ml protein)$^{-1}$ (80). Thus, the specific activity of purified ponticulin is ~112 times larger than that observed for isolated membranes, which is about the enrichment in specific activity expected for a protein that constitutes ~0.7 ± 0.4% of plasma membrane protein (103). Second, actin nucleation activity copurified with ponticulin during both gel filtration chromatography (Fig. 9 *A*) and HIC (Fig. 9 *B*). In both chromatographic steps, fractions containing the most ponticulin also exhibited the most actin nucleation activity, after reconstitution with *Dictyostelium* lipid. Because the 15- and 19-kD polypeptides are present in only trace amounts, their contributions to the total nucleation activity are unclear.

As has been documented for actin filaments nucleated by *Dictyostelium* plasma membranes (80), both ends of filaments nucleated by ponticulin appear to be available for monomer assembly and disassembly. The fast-polymerizing "barbed" ends of ponticulin-induced actin nuclei are normally free to elongate because the rate of pyrene–actin polymerization is decreased by 68 ± 21% (n = 3) in the presence of CapZ (13, 15), a protein that binds and blocks barbed filament ends (data not shown). Because this decreased rate is about the same as that observed for CapZ-nucleated actin polymerization, ponticulin-nucleated actin filaments also apparently elongate from their slow-polymerizing "pointed" ends. Accessibility of the pointed ends was confirmed by depolymerization experiments in which ponticulin-nucleated, CapZ-blocked filaments were rapidly diluted to a final actin concentration of 0.5 μM, a concentration at which depolymerization can occur only from the pointed filament ends (72). Initial depolymerization rates were linear and rapid with ~10% of the actin depolymerizing within the first minute (data not shown). Initial rates were identical for CapZ-capped filaments nucleated with (−50 ± 7 nM actin min^{-1}, n = 3) and without (−52 ± 8 nM actin min^{-1}, n = 3) ponticulin, indicating that ponticulin does not block the pointed ends of actin filaments. Thus, both the barbed and pointed ends of ponticulin-nucleated actin filaments are free.

Ponticulin Acts As a Monomer

Based on theoretical considerations, we and others have proposed that external factors may generate new membrane-associated actin nucleation sites by clustering transmembrane proteins, each with a single actin-binding site (9, 32, 77, 78). As an initial test of whether the nucleation activity of ponticulin is dependent upon dimer formation in the membrane, we assayed the nucleation activity of ponticulin reconstituted with *Dictyostelium* lipid at a wide range of lipid-to-protein ratios. In such an assay, actin assembly is expected to be linearly dependent on protein concentration for a functional monomer and to be proportional to the square of the protein concentration for a dimer in equilibrium with monomer (24). In our experiments, fold increases in the maximal rates of actin polymerization were linearly dependent on the ponticulin concentration, but essentially independent of the concentration of *Dictyostelium* lipid (Fig. 10). Similar nucle-

ation activities were observed for vesicles reconstituted from phospholipid-to-protein mole ratios varying from ~1:10 (1.4 μM phospholipid:0.5 μg/ml ponticulin) to ~6,000:1 (70 μM phospholipid:0.2 μg/ml ponticulin). Only for mole ratios exceeding $\sim 10^4$:1 (140 μM phospholipid and 0.2 or 0.3 μg/ml ponticulin) was there perhaps a deviation from linearity (not shown). These observations strongly suggest that ponticulin functions as a monomer. If dimeric ponticulin is the nucleating species, it is not in equilibrium with monomer in the range of lipid and protein concentrations used in these experiments.

The quaternary structure of ponticulin reconstituted with *Dictyostelium* lipid also was probed using water-soluble cross-linking agents. No reproducible cross-linked dimers or multimers were observed on silver-stained gels or immunoblots after treating reconstituted ponticulin with up to 20 mM 1-ethyl-3-(3-dimethylaminopropyl)carbodiimide, *m*-maleimidobenzoyl-*N*-hydroxysulfo-succinimide ester, ethylene glycol*bis*(sulfosuccinimidylsuccinate), or *bis*[2(sulfosuccinimido-oxycarbonyloxy)ethyl]sulfone (data not shown). These results indicate that, if ponticulin dimers exist, the reactive surface-accessible amino and/or sulfhydryl groups are oriented inappropriately for cross-linking by these reagents. In fact, inefficient cross-linking of ponticulin is possible because, at the highest reagent concentrations used, some cross-linking is expected even for monomers, due to random collisions in the plane of the bilayer (36).

Discussion

The ponticulin isolation procedure described here is much more efficient than the previous method in which 75–90% pure ponticulin was obtained from purified plasma membranes (103, 105). With the present procedure, essentially homogeneous ponticulin is isolated by F-actin affinity chromatography and HIC (Figs. 2 and 3, Table II) after extraction from cytoskeletons and enrichment by TX-114 phase partitioning (Fig. 1). Because the considerable time and material loss associated with plasma membrane purification (39, 47, 57) are avoided, ⩾8-fold more ponticulin is recovered per cell in about one-third the time.

Quantitative purification tables indicate that ponticulin is a relatively major component of *Dictyostelium* amebas, averaging 0.05 ± 0.01% of the total cell protein (Table I). Given that 10^{10} amebas contain ~0.5 g total protein (Table I), there is ~0.26 mg ponticulin per 10^{10} cells, or $\sim 9.1 \times 10^5$ copies/cell, with an upper estimate of 1.2×10^6 copies/cell (Table I). Thus, on a per cell basis, ponticulin is about as abundant as Band III (1.2×10^6/erythrocyte) and Thy-1 glycoprotein (1×10^6/thymocyte or neuronal cell), both of which are considered major plasma membrane proteins (10, 102).

The surface density of ponticulin also is consistent with its proposed role as a major site of cytoskeleton–membrane attachment. Assuming that 43% ($\sim 4 \times 10^5$ molecules) of the ponticulin is at the cell surface at a given time (28) and that the surface area of the *Dictyostelium* plasma membrane is ~1,400 μm²/cell (Swaisgood, M., and T. L. Steck, University of Chicago, personal communication), there are ~300 ponticulin monomers per μm² of plasma membrane. This surface density compares favorably with the 250–400 actin oligomers and ~700 ankyrins found per μm² in the erythrocyte membrane skeleton, although it is much less than the ~2,000 Band III tetramers/μm² (potential ankyrin attachment sites) (5, 10–12, 98). The surface density of ponticulin also is less than the ~1,200 molecules/μm² calculated for GPIb, the major membrane attachment site for actin-binding protein in unactivated platelets (3). (The calculation for GPIb is based on 25,000 copies/platelet and the assumption that platelets are smooth cylinders ~0.75-μm high with diameters of ~3 μm [65]). Thus, while ponticulin appears to be a major point of actin–membrane attachment in *Dictyostelium*, there is ample space on the membrane for additional cytoskeleton binding sites.

The estimated number of ponticulin monomers in the membrane is about the same as the number of short actin filaments in the cell. Based on deoxyribonuclease I inhibition assays, Podolski and Steck have reported that *Dictyostelium* amoebas contain $\sim 3.6 \times 10^5$ actin filaments with unblocked pointed ends; ~96% of these filaments average 0.22 μm in length and are proposed to populate the submembraneous cortical mesh (71). This filament number is intriguingly close to the 4×10^5 ponticulin monomers per cell estimated above.

Although limitations of the experimental approach used here have been noted (92), our hydrodynamic data (Fig. 5; Table III) indicate that ponticulin is monomeric in OG micelles. The large ν^* of the ponticulin–OG micelle appears to be attributable to the presence of the (low density) detergent and, possibly, some tightly associated lipid. These results are consistent with those reported for other integral membrane proteins, which tend to be monomers or dimers in detergent micelles containing 0.28–1.12 mg of detergent per mg protein (17, 42, 44, 76). By contrast, typical water-soluble proteins bind <0.03 mg of detergent per mg of protein (17, 44).

Detergent-solubilized ponticulin binds F-actin (Fig. 4), but does not promote actin filament assembly (Fig. 8). However, when reconstituted into *Dictyostelium* lipid vesicles (Figs. 6 and 7), highly purified ponticulin nucleates actin assembly (Fig. 8) with the activity expected if ponticulin is responsible for all the basal activity in *Dictyostelium* plasma membranes (80). Like *Dictyostelium* plasma membranes, reconstituted ponticulin nucleates actin filaments with both ends free for interactions with other proteins, including actin monomers. Activity profiles of ponticulin purified by two different methods (Fig. 9) show clearly that ponticulin is both necessary and sufficient for actin nucleation.

The dependence of nucleation activity on the presence of *Dictyostelium* lipid (Fig. 8) suggests either that ponticulin function requires a particular lipid environment or that some lipid (or proteolipid) is a cofactor. Although a need for a specific lipid is rare, the activities of many integral membrane proteins depend upon lipid composition (46, 49, 74). For instance, reconstitution of the mitochondrial proton pump is optimal in a 5:5:0.3 mix of PE/PC/cardiolipin (74), and the acetylcholine receptor does not integrate properly into bilayers lacking cholesterol (49). Clearly, the nature of the lipid(s) required for ponticulin-mediated actin nucleation is an interesting area for further investigation.

The first-order dependence of actin nucleation on ponticulin concentration over a range of protein-to-lipid ratios (Fig. 10) indicates that the actin-nucleating moiety behaves like a monomer. This result is consistent with the observation that

ponticulin in OG micelles appears to be monomeric and with the resistance of ponticulin in vesicles to chemical cross-linking. In conjunction with the previous finding that an actin trimer is the minimum assembly state required for tight binding to *Dictyostelium* plasma membranes (78), our results suggest that, like talin (50), each ponticulin molecule may promote actin nucleation by lateral stabilization of a trimeric actin nucleus. However, we cannot completely exclude the possibility that a very stable ponticulin dimer (or oligomer), resistant to chemical cross-linking, forms in the presence of *Dictyostelium* lipid.

Even if the actin-nucleating species is a ponticulin multimer with a high self-association constant in lipid bilayers, our results indicate that ponticulin-mediated actin nucleation is probably not dependent on clustering induced by extracellular factors. This conclusion is consistent with the observation that the number of actin nucleation sites is unchanged during lectin-induced capping in B-lymphocytes (48). However, the localization of nucleation sites in the plane of the membrane could be controlled by clustering ponticulin. Ponticulin function also may be regulated by upregulation from internal stores (59, 104), by oxidation and reduction of disulphide bonds (16), and/or by changes in the local lipid environment (this work). The purification and reconstitution procedures described here should potentiate the further dissection of the molecular basis for ponticulin-mediated actin nucleation which, in turn, may shed light on actin polymerization at the plasma membrane during motile processes.

We thank Dr. John Agajanian and Chris Snay of the Worcester Foundation Electron Microscope Facility for performing the electron microscopy and Dr. John Leszyck of the Worcester Foundation's W. M. Keck Protein Chemistry Facility for amino acid analyses. We also thank Drs. A. L. Hitt, H. R. Kaback, T. H. Lu, and T. L. Steck for valuable discussions and Drs. J. R. Fallon and Y.-L. Wang for a critical reading of the manuscript.

This research was supported by National Institutes of Health (NIH) grant GM33048 to E. J. Luna. This research also benefited from NIH grant CA54885 to E. J. Luna, the National Cancer Institute Cancer Center Support (Core) grant P30-12708 to the Worcester Foundation for Experimental Biology, and a grant from the J. Aron Charitable Foundation to the Worcester Foundation.

Received for publication 13 July 1992 and in revised form 13 November 1992.

References

1. Abercrombie, M. 1980. The crawling movement of metazoan cells. *Proc. R. Soc. Lond. Ser. B Biol. Sci.* 207:129–147.
2. Almog, S., B. J. Litman, W. Wimley, J. Cohen, E. J. Wachtel, Y. Barenholz, A. Ben-Shaul, and D. Lichtenberg. 1990. States of aggregation and phase transformations in mixtures of phosphatidylcholine and octyl glucoside. *Biochemistry.* 29:4582–4592.
3. Andrews, R. K., and J. E. B. Fox. 1991. Interaction of purified actin-binding protein with the platelet membrane glycoprotein Ib-IX complex. *J. Biol. Chem.* 266:7144–7147.
4. Deleted in proof.
5. Bennett, V. 1992. Ankyrins. Adaptors between diverse plasma membrane proteins and the cytoplasm. *J. Biol. Chem.* 267:8703–8706.
6. Bidlingmeyer, B. A., S. A. Cohen, and T. L. Tarvin. 1984. Rapid analysis of amino acids using pre-column derivatization. *J. Chromatogr.* 336:93–104.
7. Boggs, J. M., D. Stamp, D. W. Hughes, and C. M. Deber. 1981. Influence of ether linkage on the lamellar to hexagonal phase transition of ethanolamine phospholipids. *Biochemistry.* 20:5728–5735.
8. Bordier, C. 1981. Phase separation of integral membrane proteins in Triton X-114 solution. *J. Biol. Chem.* 256:1604–1607.
9. Brandts, J. F., and B. S. Jacobson. 1983. A general mechanism for transmembrane signaling based on clustering of receptors. *Surv. Synth. Pathol. Res.* 2:107–114.
10. Branton, D., C. M. Cohen, and J. Tyler. 1981. Interaction of cytoskeletal proteins on the human erythrocyte membrane. *Cell.* 24:24–32.
11. Bray, D. 1992. Cell Movements. Garland Publishing, Inc., New York. 406 pp.
12. Byers, T. J., and D. Branton. 1985. Visualization of the protein associations in the erythrocyte membrane skeleton. *Proc. Natl. Acad. Sci. USA.* 82:6153–6157.
13. Caldwell, J. E., S. G. Heiss, V. Mermall, and J. A. Cooper. 1989. Effects of CapZ, an actin capping protein of muscle, on the polymerization of actin. *Biochemistry.* 28:8506–8514.
14. Cantor, C. R., and P. R. Schimmel. 1980. Biophysical Chemistry, Part II. W. H. Freeman and Company, San Francisco, CA. 846 pp.
15. Casella, J. F., D. J. Maack, and S. Lin. 1986. Purification and initial characterization of a protein from skeletal muscle that caps the barbed ends of actin filaments. *J. Biol. Chem.* 261:10915–10921.
16. Chia, C. P., A. L. Hitt, and E. J. Luna. 1991. Direct binding of F-actin to ponticulin, an integral plasma membrane glycoprotein. *Cell Motil. Cytoskeleton.* 18:164–179.
17. Clarke, S. 1975. The size and detergent binding of membrane proteins. *J. Biol. Chem.* 250:5459–5469.
18. Clarke, S., and M. Smigel. 1989. Size and shape of membrane protein detergent complexes: hydrodynamic studies. *Methods Enzymol.* 172: 696–709.
19. Cocucci, S. M., and M. Sussman. 1970. RNA in cytoplasmic and nuclear fractions of cellular slime mold amoebas. *J. Cell Biol.* 45:399–407.
20. Cohen, E. J., and J. T. Edsall. 1943. Density and Apparent Specific Volumes of Proteins. *In* Proteins, Amino Acids, and Peptides. Hafner Publishing Co., Inc., New York. 370–381.
21. Cohen, S. A., B. A. Bidlingmeyer, and T. L. Tarvin. 1986. PITC derivatives in amino acid analysis. *Nature (Lond.).* 320:769–770.
22. Condeelis, J., A. Bresnick, M. Demma, S. Dharmawardhane, R. Eddy, A. L. Hall, R. Sauterer, and V. Warren. 1990. Mechanisms of amoeboid chemotaxis: an evaluation of the cortical expansion model. *Dev. Genet.* 11:333–340.
23. Cooper, J. A., S. B. Walker, and T. D. Pollard. 1983. Pyrene actin: documentation of the validity of a sensitive assay for actin polymerization. *J. Muscle Res. Cell Motil.* 4:253–262.
24. Costello, M. J., J. Escaig, K. Matsushita, P. V. Viitanen, D. R. Menick, and H. R. Kaback. 1987. Purified *lac* permease and cytochrome *o* oxidase are functional as monomers. *J. Biol. Chem.* 262:17072–17082.
25. Cullis, P. R., and M. J. Hope. 1985. Physical properties and functional roles of lipids in membranes. *In* Biochemistry of Lipids and Membranes. D. E. Vance and J. E. Vance, editors. The Benjamin/Cummings Publishing Company, Inc., Menlo Park, CA. 25–72.
26. Dabiri, G. A., J. M. Sanger, D. A. Portnoy, and F. S. Southwick. 1990. *Listeria monocytogenes* moves rapidly through the host-cell cytoplasm by inducing directional actin assembly. *Proc. Natl. Acad. Sci. USA.* 87:6068–6072.
27. Davis, A. 1984. Determination of the hydrodynamic properties of detergent-solubilized proteins. *In* Molecular and Chemical Characterization of Membrane Receptors. J C. Venter and L. C. Harrison, editors. Alan R. Liss, Inc., New York. 161–178.
28. de Chastellier, C., A. Ryter, and L. Thilo. 1983. Membrane shuttle between plasma membrane, phagosomes, and pinosomes in *Dictyostelium discoideum* amoeboid cells. *Eur. J. Cell Biol.* 30:233–243.
29. Devreotes, P. N., and S. H. Zigmond. 1988. Chemotaxis in eucaryotic cells: a focus on leukocytes and *Dictyostelium*. *Annu. Rev. Cell Biol.* 4:649–686.
30. Doren, A., and J. Goldfarb. 1970. Electrolyte effects on micellar solution of nonionic detergents. *J. Colloid Interface Sci.* 32:67–72.
31. Ebert, R. F. 1986. Amino acid analysis by HPLC: optimized conditions for chromatography of phenylthiocarbamyl derivatives. *Anal Biochem.* 154:431–435.
32. Edelman, G. M. 1976. Surface modulation in cell recognition and cell growth. *Science (Wash. DC).* 192:218–226.
33. Fleischer, B., and M. Smigel. 1978. Solubilization and properties of galactosyltransferase and sulfotransferase activities of Golgi membranes in Triton X-100. *J. Biol. Chem.* 253:1632–1638.
34. Forscher, P., and S. J. Smith. 1988. Actions of cytochalasins on the organization of actin filaments and microtubules in a neuronal growth cone. *J. Cell Biol.* 107:1505–1516.
35. Forscher, P., C. H. Lin, and C. Thompson. 1992. Novel form of growth cone motility involving site-directed actin filament assembly. *Nature (Lond.).* 357:515–518.
36. Gaffney, B. J. 1985. Chemical and biochemical crosslinking of membrane components. *Biochim. Biophys. Acta.* 822:289–317.
37. Gibbons, R. A. 1972. Physico-chemical methods for the determination of the purity, molecular size and shape of glycoproteins. *In* Glycoproteins. A. Gottschalk, editor. Elsevier, Amsterdam. 78–140.
38. Goldfarb, J., and L. Sepulveda. 1969. Application of a theory of polymer solutions to the cloud points of nonionic detergents. *J. Colloid Interface Sci.* 31:454–459.
39. Goodloe-Holland, C. M., and E. J. Luna. 1987. Purification and characterization of *Dictyostelium discoideum* plasma membranes. *Methods Cell Biol.* 28:103–128.

40. Gruner, S. M. 1985. Intrinsic curvature hypothesis for biomembrane lipid composition: a role for nonbilayer lipids. *Proc. Natl. Acad. Sci. USA.* 82:3665–3669.
41. Gruner, S. M. 1989. Stability of lyotropic phases with curved interfaces. *J. Phys. Chem.* 93:7562–7570.
42. Hackenberg, H., and M. Klingenberg. 1980. Molecular weight and hydrodynamic parameters of the adenosine 5′-diphosphate-adenosine 5′-triphosphate carrier in Triton X-100. *Biochemistry.* 19:548–555.
43. Heath, J. P. 1983. Direct evidence for microfilament-mediated capping of surface receptors on crawling fibroblasts. *Nature (Lond.).* 302:532–534.
44. Helenius, A., and K. Simons. 1972. The binding of detergents to lipophilic and hydrophilic proteins. *J. Biol. Chem.* 247:3656–3661.
45. Holloway, P. W. 1973. A simple procedure for removal of Triton X-100 from protein samples. *Anal. Biochem.* 53:304–308.
46. Houslay, M. D., and K. K. Stanley. 1982. Dynamics of Biological Membranes. Influence on Synthesis, Structure and Function. John Wiley & Sons, New York. 330 pp.
47. Ingalls, H. M., G. Barcelo, L. J. Wuestehube, and E. J. Luna. 1989. Developmental changes in protein composition and the actin-binding protein ponticulin in *Dictyostelium discoideum* plasma membranes purified by an improved method. *Differentiation.* 41:87–98.
48. Jackman, W. T., and K. Burridge. 1989. Polymerization of additional actin is not required for capping of surface antigens in B-lymphocytes. *Cell Motil. Cytoskeleton.* 12:23–32.
49. Jones, O. T., J. P. Earnest, and M. G. McNamee. 1987. Solubilization and reconstitution of membrane proteins. *In* Biological Membranes. A Practical Approach. J. B. C. Findlay and W. H. Evans, editors. IRL Press Limited, Oxford. 139–177.
50. Kaufmann, S., T. Piekenbrock, W. H. Goldmann, M. Bärmann, and G. Isenberg. 1991. Talin binds to actin and promotes filament nucleation. *FEBS (Fed. Eur. Biochem. Soc.) Lett.* 284:187–191.
51. Kouyama, T., and K. Mihashi. 1981. Fluorimetry study of *N*-(1-pyrenyl)iodoacetamide-labelled F-actin. *Eur. J. Biochem.* 114:33–38.
52. Ladbrooke, B. D., and D. Chapman. 1969. Thermal analysis of lipids, proteins and biological membranes. A review and summary of some recent studies. *Chem. Phys. Lipids.* 3:304–367.
53. Laemmli, U. K. 1970. Cleavage of structural proteins during the assembly of the head of bacteriophage T4. *Nature (Lond.).* 227:680–685.
54. Le Maire, M., L. P. Aggerbeck, C. Monteilhet, J. P. Andersen, and J. V. Moller. 1986. The use of high-performance liquid chromatography for the determination of size and molecular weight of proteins: a caution and a list of membrane proteins suitable as standards. *Anal. Biochem.* 154:525–535.
55. Lorber, B., J. B. Bishop, and L. J. DeLucas. 1990. Purification of octyl β-D-glucopyranoside and re-estimation of its micellar size. *Biochim. Biophys. Acta.* 1023:254–265.
56. Luna, E. J., V. M. Fowler, J. Swanson, D. Branton, and D. L. Taylor. 1981. A membrane cytoskeleton from *Dictyostelium discoideum.* I. Identification and partial characterization of an actin-binding activity. *J. Cell Biol.* 88:396–409.
57. Luna, E. J., C. M. Goodloe-Holland, and H. M. Ingalls. 1984. A membrane cytoskeleton from *Dictyostelium discoideum.* II. Integral proteins mediate the binding of plasma membranes to F-actin affinity beads. *J. Cell Biol.* 99:58–70.
58. Luna, E. J., L. J. Wuestehube, C. P. Chia, A. Shariff, A. L. Hitt, and H. M. Ingalls. 1990. Ponticulin, a developmentally-regulated plasma membrane glycoprotein, mediates actin binding and nucleation. *Dev. Genet.* 11:354–361.
59. Luna, E. J., L. J. Wuestehube, H. M. Ingalls, and C. P. Chia. 1990. The *Dictyostelium discoideum* plasma membrane: a model system for the study of actin-membrane interactions. *Adv. Cell Biol.* 3:1–33.
60. Maclean-Fletcher, S., and T. D. Pollard. 1980. Identification of a factor in conventional muscle actin preparations which inhibits actin filament self-association. *Biochem. Biophys. Res. Commun.* 96:18–27.
61. Marsh, D. 1990. CRC Handbook of Lipid Bilayers. CRC Press, Inc., Boca Raton, FL. 387 pp.
62. McRobbie, S. J., and P. C. Newell. 1983. Changes in actin associated with the cytoskeleton following chemotactic stimulation of *Dictyostelium discoideum. Biochem. Biophys. Res. Commun.* 115:351–359.
63. Merril, C. R., D. Goldman, S. A. Sedman, and M. H. Ebert. 1981. Ultrasensitive stain for proteins in polyacrylamide gels shows regional variation in cerebrospinal fluid proteins. *Science (Wash. DC).* 211: 1437–1438.
64. Mooseker, M. S., T. D. Pollard, and K. A. Wharton. 1982. Nucleated polymerization of actin from the membrane-associated ends of microvillar filaments in the intestinal brush border. *J. Cell Biol.* 95:223–233.
65. Nachmias, V. T., and K. Yoshida. 1988. The cytoskeleton of the blood platelet: a dynamic structure. *Adv. Cell Biol.* 2:181–211.
66. Nalecz, K. A., R. Bolli, and A. Azzi. 1986. Molecular weight estimation of membrane proteins: gel permeation chromatography and sucrose gradient centrifugation. *In* Membrane Proteins. Isolation and Characterization. A. Azzi, L. Masotti, and A. Vecli, editors. Springer-Verlag, Berlin. 11–23.
67. Okabe, S., and N. Hirokawa. 1989. Incorporation and turnover of biotin-labeled actin microinjected into fibroblastic cells: an immunoelectron microscopic study. *J. Cell Biol.* 109:1581–1595.
68. Omann, G. M., R. A. Allen, G. M. Bokoch, R. G. Painter, A. E. Traynor, and L. A. Sklar. 1987. Signal transduction and cytoskeletal activation in the neutrophil. *Physiol. Rev.* 67:285–322.
69. Parish, C. R., B. J. Classon, J. Tsagaratos, I. D. Walker, L. Kirszbaum, and I. F. C. McKenzie. 1986. Fractionation of detergent lysates of cells by ammonium sulphate-induced phase separation. *Anal. Biochem.* 156: 495–502.
70. Parkos, C. A., R. A. Allen, C. G. Cochrane, and A. J. Jesaitis. 1988. The quaternary structure of the plasma membrane β-type cytochrome of human granulocytes. *Biochim. Biophys. Acta.* 932:71–83.
71. Podolski, J. L., and T. L. Steck. 1990. Length distribution of F-actin in *Dictyostelium discoideum. J. Biol. Chem.* 265:1312–1318.
72. Pollard, T. D., and J. A. Cooper. 1986. Actin and actin-binding proteins: a critical evaluation of mechanisms and functions. *Annu. Rev. Biochem.* 55:987–1035.
73. Price, C. A. 1982. Centrifugation in Density Gradients. Academic Press, Inc., New York. 430 pp.
74. Racker, E. 1976. A New Look at Mechanisms in Bioenergetics. Academic Press, Inc., New York. 197 pp.
75. Reynolds, J. A., and D. R. McCaslin. 1985. Determination of protein molecular weight in complexes with detergent without knowledge of binding. *Methods Enzymol.* 117:41–53.
76. Sadler, J. E., J. I. Rearick, J. C. Paulson, and R. L. Hill. 1979. Purification to homogeneity of a β-galactoside α2→3 sialyltransferase and partial purification of an α-*N*-acetylgalactosaminide α2→6 sialyltransferase from porcine submaxillary glands. *J. Biol. Chem.* 254:4434–4443.
77. Schwartz, M. A., and E. J. Luna. 1986. Binding and assembly of actin filaments by plasma membranes from *Dictyostelium discoideum. J. Cell Biol.* 102:2067–2075.
78. Schwartz, M. A., and E. J. Luna. 1988. How actin binds and assembles onto plasma membranes from *Dictyostelium discoideum. J. Cell Biol.* 107:2018–209.
79. Segrest, J. P., and R. L. Jackson. 1972. Molecular weight determination of glycoproteins by polyacrylamide gel electrophoresis in sodium dodecyl sulfate. *Methods Enzymol.* 28:54–63.
80. Shariff, A., and E. J. Luna. 1990. *Dictyostelium discoideum* plasma membranes contain an actin-nucleating activity that requires ponticulin, an integral membrane glycoprotein. *J. Cell Biol.* 110:681–692.
81. Shariff, A., and E. J. Luna. 1992. Diacylglycerol-stimulated formation of actin nucleation sites at plasma membranes. *Science (Wash. DC).* 256: 245–247.
82. Shinoda, K., T. Yamaguchi, and R. Hori. 1961. The surface tension and the critical micelle concentration in aqueous solution of β-D-alkyl glucosides and their mixtures. *Bull. Chem. Soc. Jpn.* 34:237–241.
83. Siegel, L. M., and K. J. Monty. 1966. Determination of molecular weights and frictional ratios of proteins in impure systems by use of gel filtration and density gradient centrifugation. Application to crude preparations of sulfite and hydroxylamine reductases. *Biochim. Biophys. Acta.* 112:346–362.
84. Sober, H. A. 1970. Handbook of Biochemistry, 2nd Ed. The Chemical Rubber Co., Cleveland, OH.
85. Speicher, D. W. 1989. Microsequencing with PVDF membranes: efficient electroblotting, direct protein adsorption and sequencer program modifications. *In* Techniques in Protein Chemistry. T. E. Hugli, editor. Academic Press, Inc., San Diego. 24–35.
86. Spudich, J. A., and S. Watt. 1971. The regulation of rabbit skeletal muscle contraction. I. Biochemical studies of the interaction of the TM-TN complex with actin and the proteolytic fragments of myosin. *J. Biol. Chem.* 246:4866–4871.
87. Steck, T. L., and J. A. Kant. 1974. Preparation of impermeable ghosts and inside-out vesicles from human erythrocyte membranes. *Methods Enzymol.* 31:172–180.
88. Stratford, C. A., and S. Brown. 1985. Isolation of an actin-binding protein from membranes of *Dictyostelium discoideum. J. Cell Biol.* 100:727–735.
89. Svitkina, T. M., A. A. Neyfakh, Jr., and A. D. Bershadsky. 1986. Actin cytoskeleton of spread fibroblasts appears to assemble at the cell edges. *J. Cell Sci.* 82:235–248.
90. Symons, M. H., and T. J. Mitchison. 1991. Control of actin polymerization in live and permeabilized fibroblasts. *J. Cell Biol.* 114:503–513.
91. Tanford, C. 1961. Physical Chemistry of Macromolecules. John Wiley & Sons, New York. 710 pp.
92. Tanford, C., and J. A. Reynolds. 1976. Characterization of membrane proteins in detergent solutions. *Biochim. Biophys. Acta.* 457:133–170.
93. Tanford, C., Y. Nozaki, J. A. Reynolds, and S. Makino. 1974. Molecular characterization of proteins in detergent solution. *Biochemistry.* 13: 2369–2375.
94. Theriot, J. A., and T. J. Mitchison. 1991. Actin microfilament dynamics in locomoting cells. *Nature (Lond.).* 352:126–131.
95. Theriot, J. A., T. J. Mitchison, L. G. Tilney, and D. A. Portnoy. 1992. The rate of actin-based motility of intracellular *Listeria monocytogenes* equals the rate of actin polymerization. *Nature (Lond.).* 357:257–260.
96. Tilney, L. G., and S. Inoué. 1982. Acrosomal reaction of *Thyone* sperm. II. The kinetics and possible mechanism of acrosomal process elonga-

tion. *J. Cell Biol.* 93:820–827.
97. Towbin, H., T. Stahelin, and J. Gordon. 1979. Electrophoretic transfer of proteins from polyacrylamide gels to nitrocellulose sheets: procedure and some applications. *Proc. Natl. Acad. Sci. USA.* 76:4350–4354.
98. Ursitti, J. A., D. W. Pumplin, J. B. Wade, and R. J. Bloch. 1991. Ultrastructure of the human erythrocyte cytoskeleton and its attachment to the membrane. *Cell Motil. Cytoskeleton.* 19:227–243.
99. Wang, Y.-L. 1985. Exchange of actin subunits at the leading edge of living fibroblasts: possible role of treadmilling. *J. Cell Biol.* 101:597–602.
100. Weast, R. C., editor. 1969. Handbook of Chemistry and Physics. 50th ed. The Chemical Rubber Co., Cleveland, OH.
101. Weeks, G., and F. G. Herring. 1980. The lipid composition and membrane fluidity of *Dictyostelium discoideum* plasma membranes at various stages during differentiation. *J. Lipid Res.* 21:681–686.
102. Williams, A. F., and J. Gagnon. 1982. Neuronal cell Thy-1 glycoprotein: homology with immunoglobulin. *Science (Wash. DC).* 216:696–703.
103. Wuestehube, L. J., and E. J. Luna. 1987. F-actin binds to the cytoplasmic surface of ponticulin, a 17-kD integral glycoprotein from *Dictyostelium discoideum. J. Cell Biol.* 105:1741–1751.
104. Wuestehube, L. J., C. P. Chia, and E. J. Luna. 1989. Immunofluorescence localization of ponticulin in motile cells. *Cell Motil. Cytoskeleton.* 13:245–263.
105. Wuestehube, L. J., D. W. Speicher, A. Shariff, and E. J. Luna. 1991. F-actin affinity chromatography of detergent-solubilized plasma membranes: purification and initial characterization of ponticulin from *Dictyostelium discoideum* plasma membranes. *Methods Enzymol.* 196: 47–65.
106. Yedgar, S., Y. Barenholz, and V. G. Cooper. 1974. Molecular weight, shape and structure of mixed micelles of Triton X-100 and sphingomyelin. *Biochim. Biophys. Acta.* 363:98–111.
107. Yuen, S. W., A. H. Chui, K. J. Wilson, and P. M. Yuan. 1988. Microanalysis of SDS-PAGE electroblotted proteins. *Applied Biosystems Inc. User Bulletin.* 36:8–9.